Approximation of Transmission Line Parameters of Single-core and Three-core XLPE Cables

P. Wagenaars, P. A. A. F. Wouters
Eindhoven University of Technology
Faculty of Electrical Engineering, Electrical Power Systems
P.O. Box 513, 5600 MB Eindhoven, The Netherlands

P. C. J. M. van der Wielen and **E. F. Steennis**
KEMA
P.O. Box 9035, 6800 ET Arnhem, The Netherlands

ABSTRACT

A transmission line model of a power cable is required for the analysis of the behavior of high-frequency phenomena, such as partial discharges, lightning impulses and switching transients, in cables. A transmission line is characterized by its characteristic impedance, attenuation coefficient and propagation velocity. The semiconducting layers in an XLPE cable have a significant influence on these parameters. Unfortunately, the dielectric properties of these layers are usually unknown and can differ between similar types of cables. In this paper it is shown that nevertheless the characteristic impedance and propagation velocity of single-core and three-core XLPE cables can be estimated using available information from the cable specifications. The estimated values are validated using pulse response measurements on cable samples.

Index Terms — **Cross-linked polyethylene insulation, modeling, (multiconductor) transmission lines, parameter estimation, power cables.**

1 INTRODUCTION

PARTIAL discharges (PDs), lightning impulses, switching transients and breakdowns have in common that they result in high-frequency signals traveling through the network. A model that describes the propagation of these signals through cable systems is essential for the understanding and analysis of these phenomena.

A power cable can be modeled as a transmission line to describe its behavior for high-frequency transients. A transmission line is fully specified by two parameters: the characteristic impedance Z_c and the propagation coefficient γ. The propagation coefficient contains both signal attenuation α and propagation velocity v_p. For single-core XLPE cables accurate models have been developed [1-4]. These models require detailed information on the cable construction and material properties. Unfortunately, not all required parameters are readily available, especially the dielectric properties at high-frequencies of the semiconducting layers are hard to obtain.

This paper describes how the characteristic impedance Z_c and the propagation velocity v_p can be approximated with solely input parameters that are easily accessible. Furthermore, this approach is extended to three-core XLPE cable constructions.

Manuscript received on 11 February 2009, in final form 18 August 2009.

2 CABLE CONSTRUCTION

Cable design parameters from both a single-core cable and a three-core cable are studied in this section.

2.1 SINGLE-CORE XLPE CABLE

The cross-section of a typical single-core XLPE cable is depicted in Figure 1. The cable consists of the following layers:

- Conductor, aluminum or copper conductor with radius r_c.
- Conductor screen, semiconducting layer extruded around conductor with thickness t_{cs} and complex permittivity $\varepsilon_{r,cs}$ ($= \varepsilon'_{r,cs} - j\varepsilon''_{r,cs}$).

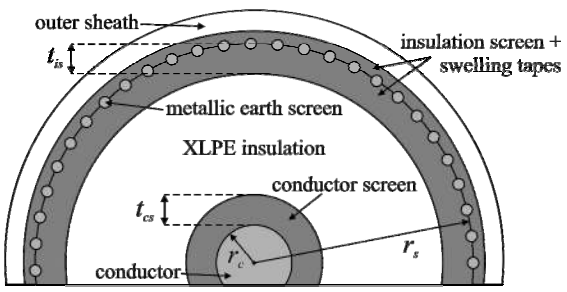

Figure 1. Schematic drawing of a typical single-core XLPE cable. Light gray: metallic parts (i.e. conductor and earth screen), dark gray: semiconducting layers (i.e. conductor screen, insulation screen and swelling tapes).

- Insulation, most modern MV and HV cables use XLPE with complex relative permittivity $\varepsilon_{r,insu}$ ($= \varepsilon'_{r,insu} - j\varepsilon''_{r,insu}$).
- Insulation screen, semiconducting layer around insulation with thickness t_{is} and complex relative permittivity $\varepsilon_{r,is}$ ($= \varepsilon'_{r,is} - j\varepsilon''_{r,is}$).
- Swelling tapes, many modern cables have semiconducting swelling tapes wrapped around the insulation screen. Because the electrical properties of this layer are similar to the insulation screen [3], we consider these layers as one.
- Earth screen with inner radius r_s. Construction of this metallic screen depends on cable type. An often-used construction consists of copper wires wrapped helically around the cable. These wires are held in place by a counter-wound copper tape. Another construction, sometimes used, involves an aluminum foil earth screen. This paper deals with both these constructions.
- Outer sheath, usually polyethylene (PE), has no influence on the characteristic impedance and propagation coefficient.

2.2 THREE-CORE XLPE CABLE

There are various constructions of three-core XLPE cables. Each core can be equipped with a metallic earth screen. From a transmission-line-modeling point of view each core in this type of cable behaves effectively as a separate single-core cable. The design considered in this paper requires a more extensive model. This design does not apply a metallic earth screen around individual cores. Instead, each separate core is only equipped with a semiconducting insulation screen and swelling tapes and a single earth screen is applied around the composition of all three cores. A schematic drawing is depicted in Figure 2. It consists of the following parts:

- Each core has:
  - Conductor with radius r_c.
  - Conductor screen, semiconducting layer extruded around conductor with thickness t_{cs} and complex permittivity $\varepsilon_{r,cs}$ ($= \varepsilon'_{r,cs} - j\varepsilon''_{r,cs}$).
  - Insulation, usually XLPE, with outer radius r_{insu} and complex relative permittivity $\varepsilon_{r,insu}$ ($= \varepsilon'_{r,insu} - j\varepsilon''_{r,insu}$).
  - Insulation screen, a semiconducting layer around insulation with thickness t_{is} and complex relative permittivity $\varepsilon_{r,is}$ ($= \varepsilon'_{r,is} - j\varepsilon''_{r,is}$).
  - Swelling tapes, in this paper considered to be part of the insulation screen.
- Filler, the space between the cores is filled with a filling material. This material has virtually no influence on the transmission line parameters of the cable.
- Swelling tapes, semiconducting swelling tapes cover all three cores and the filler.
- Metallic earth screen with inner radius r_s. This screen usually consists of helically wound copper wires.
- Outer sheath, usually PE, has no influence on the transmission line parameters.

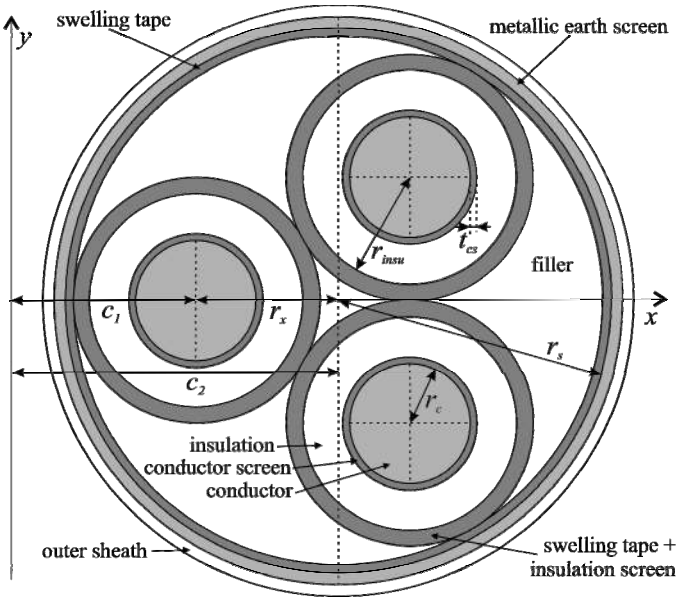

Figure 2. Schematic drawing of three-core XLPE cable with common earth screen. Light gray: metallic parts (i.e. conductors and earth screen), dark gray: semiconducting layers (i.e. conductor screen, insulation screen and swelling tapes).

3 TRANSMISSION LINE PARAMETERS

For high frequencies ($f >> v_p$ / cable length) a coaxial structure such as a power cable can be modeled as a transmission line. A single-core cable can be described as a two-conductor (conductor and earth screen) transmission line (2TL) and a three-core cable as a multiconductor transmission line (MTL). Transmission line theory can be found in general textbooks such as [5-6].

3.1 TWO-CONDUCTOR TRANSMISSION LINE

A 2TL can be described in terms of the distributed series impedance Z and the distributed shunt admittance Y. These parameters are expressed in terms of the resistance R, inductance L, conductance G and (complex) capacitance C:

$$Z(\omega) = R(\omega) + j\omega L(\omega) \quad \text{and} \quad Y(\omega) = G(\omega) + j\omega C(\omega) \tag{1}$$

For an EM wave that propagates through the cable the ratio between voltage and current is given by the characteristic impedance Z_c:

$$Z_c(\omega) = \sqrt{\frac{Z(\omega)}{Y(\omega)}} \tag{2}$$

The propagation and distortion of a wave traveling through a transmission line is described by the propagation coefficient γ:

$$\gamma(\omega) = \sqrt{Z(\omega) \cdot Y(\omega)} = a(\omega) + j\beta(\omega) \tag{3}$$

The real part of γ is the attenuation coefficient α. This frequency dependent parameter describes the attenuation due to losses as waves propagate through the transmission line. The propagation velocity v_p can be obtained from the imaginary part of γ:

$$v_p(\omega) = \frac{\omega}{\beta(\omega)} \tag{4}$$

3.2 MULTICONDUCTOR TRANSMISSION LINE

A three-core cable with common earth screen, as shown in Figure 2, has four conducting parts. The common earth screen is the reference/ground conductor. The voltages on and currents through the three conductors are defined as:

$$\mathbf{V} = (V_1, V_2, V_3)^T \tag{5}$$

$$\mathbf{I} = (I_1, I_2, I_3)^T \tag{6}$$

where V_i is the voltage (relative to the earth screen) on the i^{th} conductor and I_i is the current through the i^{th} conductor.

The per-unit-length impedance matrix **Z** is a 3-by-3 matrix with self-impedances (Z_s) on the diagonal and mutual impedances (Z_m) off-diagonal. Due to symmetry in a three-core cable the three self-impedances are equal and all mutual impedances are equal. For the admittance matrix **Y** the same symmetry considerations apply:

$$\mathbf{Z} = \begin{pmatrix} Z_s & Z_m & Z_m \\ Z_m & Z_s & Z_m \\ Z_m & Z_m & Z_s \end{pmatrix} \quad \text{and} \quad \mathbf{Y} = \begin{pmatrix} Y_s & Y_m & Y_m \\ Y_m & Y_s & Y_m \\ Y_m & Y_m & Y_s \end{pmatrix} \tag{7}$$

The self and mutual impedances and admittances Z_s, Z_m, Y_s and Y_m can be expressed in terms of resistance, inductance, conductance and capacitance:

$$\begin{aligned} Z_s &= R_s + j\omega L_s \quad \text{and} \quad Z_m = R_m + j\omega L_m \\ Y_s &= G_s + j\omega C_s \quad \text{and} \quad Y_m = G_m + j\omega C_m \end{aligned} \tag{8}$$

The general solution is most conveniently decoupled using a transformation matrix **T** to obtain the modal solutions [7]. The modal solution consists of propagation modes that are independent of each other. Since **Z** and **Y** of a three-core power cable are cyclic symmetric the transformation matrix becomes:

$$\mathbf{T} = \frac{1}{\sqrt{3}} \begin{pmatrix} 1 & 1 & 1 \\ 1 & e^{j\frac{2}{3}\pi} & e^{j\frac{1}{3}\pi} \\ 1 & e^{j\frac{4}{3}\pi} & e^{j\frac{2}{3}\pi} \end{pmatrix} \tag{9}$$

The expression for the resulting modal voltages $\mathbf{V_m}$ and currents $\mathbf{I_m}$ in terms of the normal voltages **V** and currents **I** can be found in the appendix. The modal solutions can be interpreted as a shield-to-phase (SP) propagation mode and two phase-to-phase (PP) modes. For the SP propagation mode the three-conductors can be regarded as one conductor of a 2TL, and the earth screen as the return conductor. We define the voltage V_{sp} and current I_{sp} of the SP mode as:

$$\begin{aligned} V_{sp} &\equiv \tfrac{1}{3}(V_1 + V_2 + V_3) \\ I_{sp} &\equiv I_1 + I_2 + I_3 \end{aligned} \tag{10}$$

The two PP modes can be interpreted as a mode traveling between conductor 1 and 2, and a mode between conductor 1 and 3. The mode between conductor 2 and 3 is a linear combination of these two. We define the voltage and current of the first PP channel as:

$$\begin{aligned} V_{pp,1} &\equiv V_1 - V_2 \\ I_{pp,1} &\equiv \tfrac{1}{2}(I_1 - I_2) \end{aligned} \tag{11}$$

The expressions for voltage $V_{pp,2}$ and current $I_{pp,2}$ of the second PP channel are similar to equation (11) except that V_2 and I_2 have to be replaced by respectively V_3 and I_3. The transmission line parameters of the SP and PP channel, as defined above, can be expressed in terms of the mutual and self impedances and admittances (appendix).

$$Z_{sp} = \frac{1}{3}\sqrt{\frac{2Z_m + Z_s}{2Y_m + Y_s}} \tag{12}$$

$$Z_{pp} = 2\sqrt{\frac{Z_m - Z_s}{Y_m - Y_s}} \tag{13}$$

$$\gamma_{sp} = \sqrt{(2Z_m + Z_s)(2Y_m + Y_s)} \tag{14}$$

$$\gamma_{pp} = \sqrt{(Z_m - Z_s)(Y_m - Y_s)} \tag{15}$$

4 PARAMETER APPROXIMATIONS

Theoretical models of transmission line parameters, e.g. [1-4], require detailed knowledge of the cable parameters. Generally, the cable manufacturer can supply most of them, but not all. Especially, the complex relative permittivity ε_r of the semiconducting layers at high frequencies is usually not available. Accurate measurement of ε_r is possible, but complicated [3, 8]. Approximations of the transmission line parameters, using only information that is readily available from the cable manufacturer, are described in this section.

4.1 SINGLE-CORE CABLE

4.1.1 CHARACTERISTIC IMPEDANCE

The series impedance Z is primarily determined by the inductance L and the shunt admittance Y by C. Assuming $Z = j\omega L$ and $Y = j\omega C$ equation (2) reduces to:

$$Z_c(\omega) = \sqrt{\frac{L(\omega)}{C(\omega)}} \tag{16}$$

Substitution of L and C with their equations for a coaxial structure yields:

$$Z_c(\omega) = \frac{1}{2\pi}\sqrt{\frac{\mu_0\mu_r}{\varepsilon_0\varepsilon_r(\omega)}}\ln\left(\frac{r_s}{r_c}\right) \tag{17}$$

The relative permeability μ_r of the insulation and semiconducting layers is equal to one. The complex relative permittivity of the insulation $\varepsilon_{r,insu}$ differs from the relative permittivity of the conductor screen $\varepsilon_{r,cs}$ and the insulation screen $\varepsilon_{r,is}$. Therefore, ε_r in equation (17) is replaced by an effective permittivity $\varepsilon_{r,eff}$. This is the relative permittivity of the homogeneous insulation material of a fictive coaxial capacitor with the same total capacitance and inner and outer radius (respectively r_c and r_s). The capacitance of a single-core XLPE cable with semiconducting screens is a series of three (complex) capacitances: C_{cs} for the conductor screen, C_{insu} for the XLPE insulation, and C_{is} for the insulation screen. Figure 3 depicts the capacitances of the insulation and semiconducting layers and their relation to the effective capacitance C_{eff}.

For frequencies up to at least several tens of MHz C_{insu} is much smaller than C_{cs} and C_{is} because (i) the relative permittivity (both ε'_r and ε''_r) of the semiconducting layers is much larger than for XLPE [3, 8-9], and (ii) the insulation is much thicker. Therefore, $C_{cs} >> C_{insu}$ and $C_{is} >> C_{insu}$, and thus $C_{eff} \approx C_{insu}$. Because XLPE has extremely low losses $\varepsilon_{r,insu} \approx \varepsilon'_{r,insu}$. The effective relative permittivity can therefore be expressed in terms of $\varepsilon'_{r,insu}$ and the dimensions:

$$\frac{2\pi\varepsilon_0\varepsilon_{r,eff}(\omega)}{\ln\left(\frac{r_s}{r_c}\right)} \approx \frac{2\pi\varepsilon_0\varepsilon'_{r,insu}(\omega)}{\ln\left(\frac{r_s - t_{is}}{r_c + t_{cs}}\right)}$$
$$\varepsilon_{r,eff}(\omega) \approx \varepsilon'_{r,insu}(\omega)\frac{\ln\left(\frac{r_s}{r_c}\right)}{\ln\left(\frac{r_s - t_{is}}{r_c + t_{cs}}\right)} \tag{18}$$

This equation shows that $\varepsilon_{r,eff}$ is always larger than $\varepsilon'_{r,insu}$. For a typical 240 mm^2 6/10 kV cable where $r_c = 9.0$ mm, $t_{cs} = 0.7$ mm, $t_{is} = 0.7$ mm and $r_s = 13.8$ mm $\varepsilon_{r,eff}$ is 1.42× $\varepsilon'_{r,insu}$. Note that for XLPE insulation $\varepsilon'_{r,insu}$ is frequency-independent for the frequency range up to several tens of MHz, the range required for most diagnostic tools applied on power cables [10].

Combining equations (17) and (18) yields:

$$Z_c(\omega) \approx \frac{1}{2\pi}\sqrt{\frac{\mu_0}{\varepsilon_0\varepsilon_{r,eff}}\ln\left(\frac{r_s}{r_c}\right)}$$
$$\approx \frac{1}{2\pi}\sqrt{\frac{\mu_0}{\varepsilon_0\varepsilon'_{r,insu}}\ln\left(\frac{r_s}{r_c}\right)\ln\left(\frac{r_s - t_{is}}{r_c + t_{cs}}\right)} \tag{19}$$

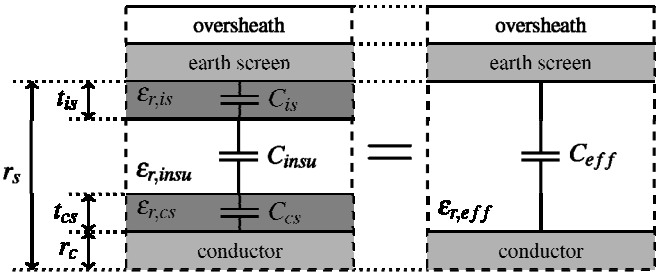

Figure 3. Relation between the complex capacitances $C_{cs} - C_{insu} - C_{is}$ and C_{eff}.

4.1.2 PROPAGATION VELOCITY

The propagation velocity is determined by the imaginary part β of the propagation coefficient. The β is predominantly determined by the inductance and capacitance. Therefore, we assume $Z = j\omega L$ and $Y = j\omega C$. This reduces equation (3) to:

$$\gamma(\omega) = \sqrt{j\omega L(\omega)\cdot j\omega C(\omega)} = j\omega\sqrt{L(\omega)C(\omega)} \tag{20}$$

The propagation velocity can be approximated by:

$$v_p(\omega) = \frac{1}{\sqrt{L(\omega)C(\omega)}} \tag{21}$$

For homogeneous media $LC = \varepsilon_0\varepsilon_r\mu_0\mu_r$ [6]. However, the material between conductor and (wire) screen is not homogeneous. Therefore, ε_r has to be replaced $\varepsilon_{r,eff}$ as derived in equation (18).

If the cable has a helical wire screen the velocity v_p is also affected by the helical lay of the wire screen. The conductive current over the individual wires of the screen can hardly cross over. The charges of a pulse in the wire tend to follow the helical lay [11, 12]. Therefore, the pulse must travel a longer distance, resulting in a lowered velocity along the cable axis. Assuming a helical wire screen with a "large" number of wires (> 10), sufficiently low frequencies (below several tens of MHz), and a straight conductor the correction factor F_{hl} for the velocity is given by [11]:

$$F_{hl} = \frac{1}{\sqrt{1 + \left(\frac{2\pi r_s}{l_l}\right)^2 \cdot \frac{1 - (r_c/r_s)^2}{2\ln(r_s/r_c)}}} \tag{22}$$

with l_l the lay length, this is the longitudinal distance along the cable required for one complete helical wrap of one wire. Note that F_{hl} is always larger (i.e. closer to 1) than the extra length of the helical lay relative to the axial length would result in directly. This is in agreement with the simulation in [12]. From this observation, it is apparent that the pulses do not completely follow the helical lay of the wire screen.

Note that equation (22) does not take into account the following aspects:

- Semi-conducting layers. The presence of semi-conducting layers may have an influence on the factor F_{hl}

because charges can transfer from one wire to another more easily.

- Stranded core conductors. These strands also have a helical lay. Usually, the helical lay length of the conductor strands is much shorter than the lay length of the wire screen, but the capacitive/conductive coupling between these wires is much stronger than between the earth screen wires. Therefore, the helical lay of conductor strands has negligible influence on the propagation velocity.
- Some wire screens with a helical lay do not have a constant angle between wire and cable axis. Instead, the lay angle goes back and forth. In this situation correction factor is expected to be between the value for a helical screen given by equation (22) and 1 if no helical screen is present.

Combining equations (18), (21) and (22) the velocity can be approximated with:

$$v_p(\omega) \approx \frac{c}{\sqrt{\varepsilon_{r,eff}}} F_{hl} \approx \frac{c}{\sqrt{\varepsilon'_{r,insu}(\omega)}} \sqrt{\frac{\ln\left(\frac{r_s - t_{is}}{r_c + t_{cs}}\right)}{\ln\left(\frac{r_s}{r_c}\right)}} F_{hl} \quad (23)$$

where c is the speed of light in vacuum ($c = 1/\sqrt{\varepsilon_0 \mu_0}$). For cables with an aluminum foil earth screen the factor F_{hl} must be omitted. Note that v_p is independent of the frequency if $\varepsilon'_{r,insu}$ is frequency-independent, which is true for XLPE.

4.1.3 ATTENUATION

For convenience, the dielectric losses (described by ε''_r) are incorporated into G, making C real-valued. The attenuation is determined by the real part of the propagation velocity. Therefore, R and G must be taken into account for the calculation of the attenuation. Assuming $R << \omega L$ and $G << \omega C$ yields in combination with equation (3):

$$\alpha(\omega) \approx \frac{1}{2}\left(R(\omega)\sqrt{\frac{C(\omega)}{L(\omega)}} + G(\omega)\sqrt{\frac{L(\omega)}{C(\omega)}} \right) = \alpha_R(\omega) + \alpha_G(\omega) \quad (24)$$

The attenuation is split in two parts: α_R and α_G. The first part, α_R, is the attenuation caused by losses in the conductor and earth screen. Due to the skin effect, the conductor and earth screen resistances are proportional to the square root of the frequency, and scale as $\alpha_R \propto \sqrt{\omega}$. The second part, α_G, is caused by the losses in the insulation and semi-conducting layers. Since XLPE has a very small loss tangent the losses in the semi-conducting screens are dominant. Due to the large variation in the properties of the semiconducting layers [3, 8] it is not possible to estimate the attenuation with reasonable accuracy without knowledge of the exact properties of the semiconducting layers of the cable under test.

4.2 THREE-CORE CABLE

In order to calculate the characteristic impedance and propagation coefficient of the SP and PP channel the self-impedance/admittance (Z_s and Y_s) of each phase and the mutual-impedance/admittance between phases (Z_m and Y_m) are required. Again we assume that the impedances are dominated by the inductances: $Z_s = j\omega L_s$ and $Z_m = j\omega L_m$. And that the admittances are dominated by the capacitances: $Y_s = j\omega C_s$ and $Z_m = j\omega C_m$.

Next, the values for L_s, L_m, C_s and C_m have to be determined. These parameters can be estimated using numerical methods, such as the boundary element method (BEM) [13]. The main disadvantage of this method is that it requires dedicated software. Another option is to estimate the parameters analytically using conformal mapping [14-15].

4.2.1 BEM ESTIMATION

In order to determine the self- and mutual capacitances conductor i is set to 1 V, while the other conductors are set to 0 V. From the electric field distribution the associated charge on each conductor j is determined, which is equal to the capacitance c_{ij}. The inductances can be determined in a similar fashion by sending a current of 1 A through the i^{th} conductor, 0 A through the other conductors. From the simulated magnetic flux the inductance matrix can be constructed. Alternatively, if the cable does not contain any components with a $\mu_r \neq 1$ the inductance matrix $\mathbf{L}$ can be directly obtained from the free-space capacitance matrix $\mathbf{C_0}$ (capacitance matrix when ε_r of all materials is set to 1). The relation $\mathbf{L} = \mu_0 \varepsilon_0 \mathbf{C_0}^{-1}$ can be applied to calculate the inductance matrix. The resulting $\mathbf{L}$ and $\mathbf{C}$ can be converted to the characteristic impedance and propagation velocity for both propagation modes using equations (12)-(15).

4.2.2 CONFORMAL MAPPING ESTIMATION

The analytical method used in [14-15] uses a conformal transformation to calculate the capacitances and inductances for a metallic pipe with eccentric conductors. The transformation maps the orthogonal coordinate system to another coordinate system for which a closed form solution is available. The method assumes that the second and third conductor have no influence on the magnetic field lines resulting from a current through the first conductor. If the conductors are small relative to the radius of the metallic screen this assumption holds. For a typical power cable this approximation does not really apply, but nonetheless, the method may provide indicative values with sufficient accuracy for parameter estimation. In [16] a more accurate analytical method derived from Poynting's theorem is described. This method, however, is computationally intensive, and therefore provides little advantage over the BEM estimation.

The conformal mapping is given by:

$$x' + jy' = \frac{x + jy - s}{x + jy + s} \quad (25)$$

where x and y are the orthogonal x- and y-coordinate, x' and y' are the x- and y-coordinate after transformation, and s is a parameter that is chosen such that after transformation the eccentric conductor and earth screen become concentric. The parameter s is calculated using:

$$c_1 = \frac{r_s^2 - r_c^2 - r_x^2}{2r_x} \tag{26}$$

$$s^2 = c_1^2 - r_c^2 \tag{27}$$

where r_x is the distance from the center of a conductor to the center of the entire cable, and c_1 the x-coordinate of the center of the first conductor. See also Figure 2 for the definition of these parameters. The conductor radius, earth screen radius, and distance from cable center to center of the 2nd and 3rd conductor after transformation (respectively R_c, R_s and R_x) are given by:

$$c_2 = \frac{r_s^2 - r_c^2 + r_x^2}{2r_x} = c_1 + r_x \tag{28}$$

$$R_c = \frac{r_c}{c_1 + s} \tag{29}$$

$$R_s = \frac{r_s}{c_2 + s} \tag{30}$$

$$R_x = \sqrt{\frac{(c_2 + \frac{1}{2}r_x - s)^2 + \frac{3}{4}r_x^2}{(c_2 + \frac{1}{2}r_x + s)^2 + \frac{3}{4}r_x^2}} \tag{31}$$

Compared to the conductors and the earth screen the semiconducting screens and swelling tapes have a negligible conductivity. Their influence on the self- and mutual inductances is negligible. The self- and mutual-inductances are given by:

$$L_s = \frac{\mu_0}{2\pi}\ln\left(\frac{R_s}{R_c}\right) \tag{32}$$

$$L_m = \frac{\mu_0}{2\pi}\ln\left(\frac{R_s}{R_x}\right) \tag{33}$$

A three-core XLPE cable with common earth screen does not have a metallic screen around each core, but each core is enclosed by a semiconducting insulation screen. The impedance of the semiconducting screen is low compared to the impedance of the XLPE insulation. The swelling tapes, which are between the insulation screen and the metallic earth screen are also semiconducting. Therefore, the insulation screen around each core has approximately the same potential as the earth screen and the total voltage drops across the XLPE insulation. This results in a straightforward calculation of the admittance matrix **Y**. The self-capacitance C_s is given by the equation for a single-core coaxial capacitance. The mutual capacitance C_m is equal to zero because of the screening by the semiconducting insulation screens:

$$C_s = \frac{2\pi\varepsilon_0\varepsilon'_{r,insu}}{\ln\left(\frac{r_{insu}}{r_c + t_{cs}}\right)} \tag{34}$$

$$C_m = 0 \tag{35}$$

where r_{insu} is the outer radius of the insulation.

5 EXPERIMENT

In order to validate the model approximations pulse response measurements [17] have been performed on three cables: two single-core cables and a three-core cable with common earth screen. The measured characteristic impedance and propagation velocity are compared with the approximations.

5.1 SINGLE-CORE CABLE

The dimensions of the two examined MV single-core XLPE cables are summarized in Table 1. These values are taken directly from the cable's datasheet or are derived from those values. The value for the lay length for cable 2 was not mentioned. A typical lay length of 8× the shield diameter is taken. Approximate values for the characteristic impedance and propagation velocity are calculated using equations (19) and (23).

The experimental results and the approximation of cable 1 are plotted in Figure 4 and Figure 5. The results of cable 2 are depicted in Figure 6 and Figure 7. The "peaks" around 9 MHz are measurement artifacts caused by the fact that the injected pulse is a square pulse with a width of 110 ns. It has no energy content for that frequency. The figures show that Z_c and v_p are estimated with an accuracy of about 5%.

5.2 THREE-CORE CABLE

The dimensions of the three-core XLPE cable are listed in Table 2. The transmission line parameters of the SP channel and the PP channel are determined using two measurements. In the first measurement the three conductors are connected together and a pulse is injected between the earth screen and the three conductors. This measurement yields the SP parameters Z_{sp} and γ_{sp}. For the second measurement two conductors are floating and a pulse is injected between the

Table 1. Single-core cables used in tests.

	Cable 1	Cable 2
Conductor radius (r_c)	10.3 mm	10.25 mm
Thickness of conductor screen (t_{cs})	0.7 mm	0.95 mm
Relative permittivity of insulation ($\varepsilon'_{r,insu}$) [10, 18]	2.26	2.26
Thickness of insulation screen (t_{is})	1.1 mm	1.25 mm
Earth screen radius (r_s)	15.6 mm	16.05 mm
Lay length (l_l)	N/A (Al tape screen)	257 mm
Cable length	138 m	519.6 m

Table 2. Three-core cable used in tests

	Cable 3
Conductor radius (r_c)	8.55 mm
Thickness of conductor screen (t_{cs})	0.8 mm
Outer radius insulation (r_{insu})	12.75 mm
Rel. permittivity of insulation ($\varepsilon'_{r,insu}$) [10, 18]	2.26
Distance core center to cable center (r_x)	16.13 mm
Earth screen radius (r_s)	30.5 mm
Cable length	350.9 m

third conductor and the earth screen. This injects a pulse in both the SP and the PP channel. The resulting transmission line parameters Z_{ssp} and γ_{ssp} are therefore a combination of the SP and PP channel parameters. The ratio of the voltage and current of a single phase Z_{ssp} is equal to any diagonal element of $\mathbf{T}\cdot\mathbf{Z_{cm}}\cdot\mathbf{T}^{-1}$ (see appendix (43)).

$$Z_{pp} = 3(Z_{ssp} - Z_{sp}) \tag{36}$$

Similarly, the effective propagation factor $\exp(-\gamma_{ssp}\cdot z)$ of a one phase signal after propagation over a distance z can be defined as the diagonal element of $\mathrm{T}\cdot\exp(\gamma_m\ z)\cdot\mathrm{T}^{-1}$ (see appendix (47)).

$$\mathrm{e}^{-\gamma_{pp}z} = \tfrac{1}{2}\left(3\,\mathrm{e}^{-\gamma_{ssp}z} - \mathrm{e}^{-\gamma_{sp}z}\right) \tag{37}$$

The characteristic impedance and propagation velocity of the measured cable are estimated using the BEM and conformal mapping methods. The measured and estimated Z_c and v_p of the SP channel are plotted in Figure 8 and Figure 9. The Z_c and v_p of the PP channel are plotted in Figure 10 and Figure 11. The "peaks" around 9 MHz are again the same measurement artifacts as explained before. Above 7-8 MHz the measured propagation velocity is unreliable due to the lack of energy in the reflected pulses at high frequencies.

The figures show that the estimates of the characteristic impedance of both the SP and the PP channel are less accurate than for the single-core cables. The BEM model is slightly more accurate than the conformal mapping estimation. For the propagation velocity the BEM method deviates approximately

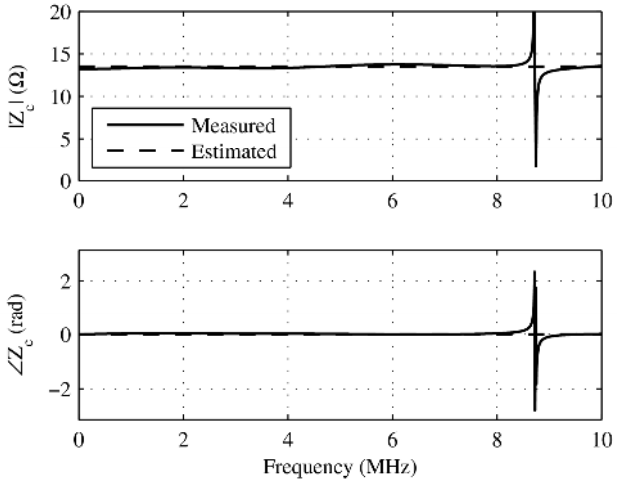

Figure 4. Measured and estimated characteristic impedance of cable 1

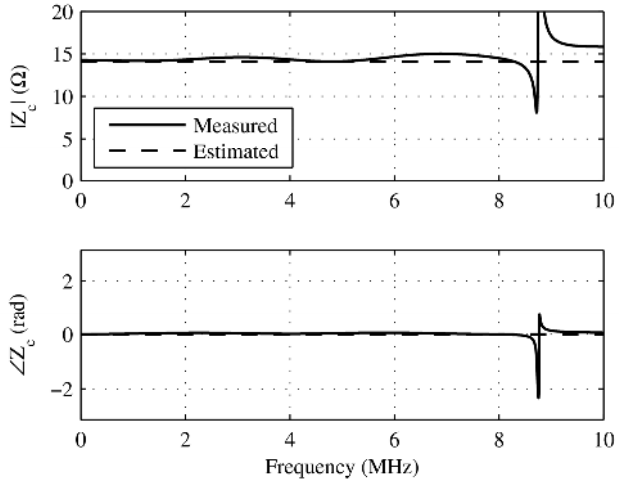

Figure 6. Measured and estimated characteristic impedance of cable 2.

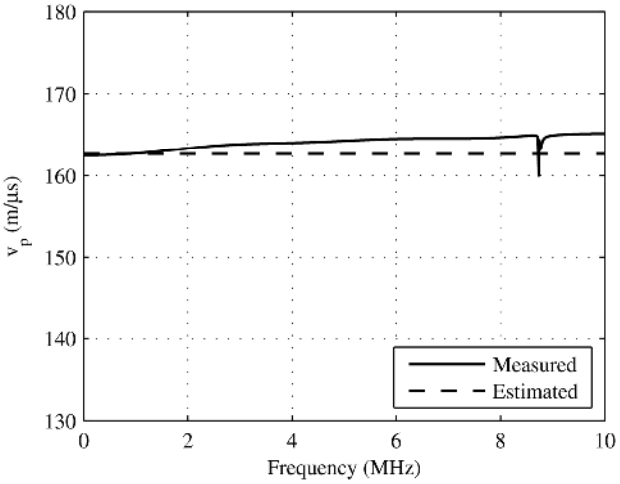

Figure 5. Measured and estimated propagation velocity of cable 1.

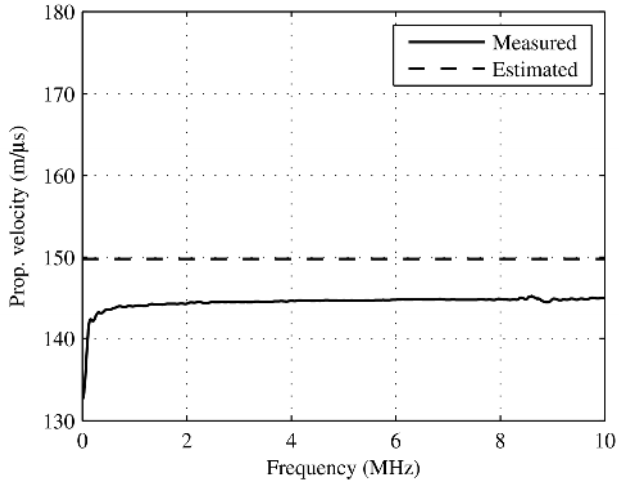

Figure 7. Measured and estimated propagation velocity of cable 2.

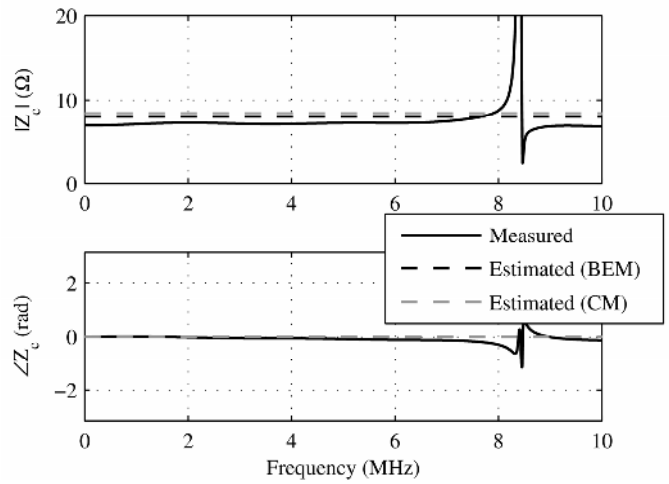

Figure 8. Measured and estimated (using BEM and conformal mapping) characteristic impedance of SP channel of cable 3.

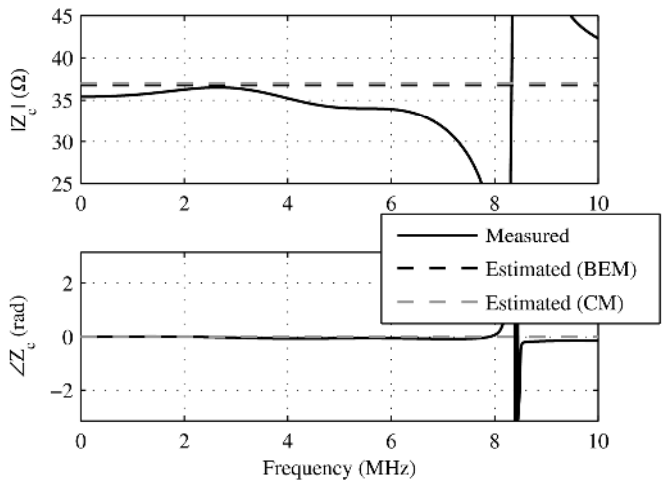

Figure 10. Measured and estimated (using BEM and conformal mapping) characteristic impedance of PP channel of cable 3.

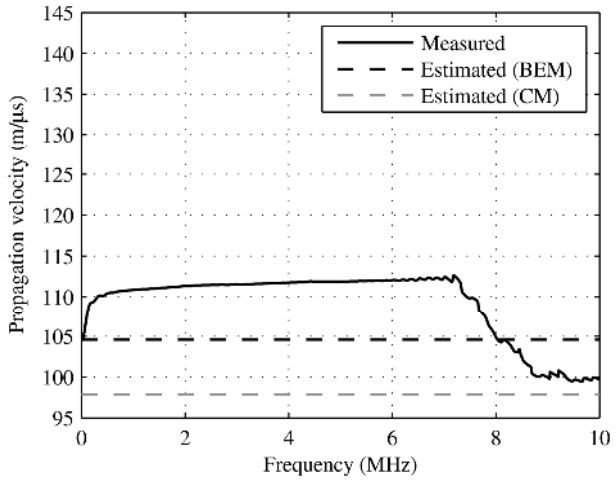

Figure 9. Measured and estimated (using BEM and conformal mapping) propagation velocity of SP channel of cable 3.

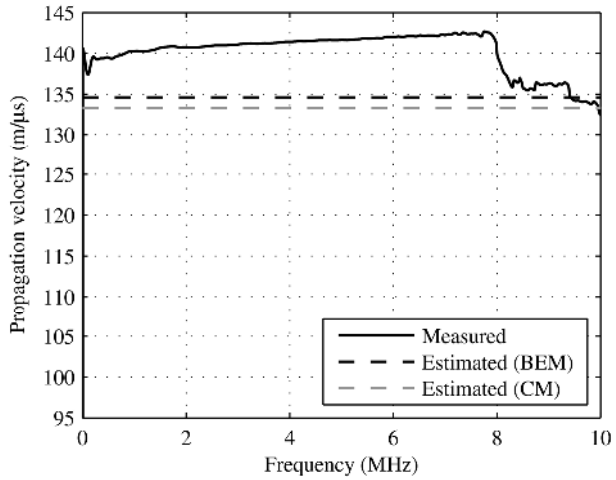

Figure 11. Measured and estimated (using BEM and conformal mapping) propagation velocity of PP channel of cable 3.

5%, while the conformal mapping shows an accuracy of 5 to 15%.

6 DISCUSSION

The value of the presented models does not only depend on the accuracy of the model itself, but also on the uncertainty of the input parameters. An extensive analysis of the sensitivity of the transmission line parameters to uncertainties in the input parameters is presented in [19] for single-core cables. From this analysis the sensitivity of Z_c and v_p to changes in the input parameters is plotted in Figure 12 and Figure 13. The figures show that Z_c and v_p are relatively insensitive to changes in t_{cs} and t_{is}. A change of 10% in these thicknesses results in a less than 1% change in Z_c and v_p. The transmission line parameters are more sensitive to changes in r_c and r_s (a 5% change in these input parameters results in a 10% change Z_c and maximal a 5% change in v_p). However, the inner and outer conductor radii are generally specified more precise than the thickness of the semiconducting layers. The relative uncertainty in the radii is in the order of 1%, whereas the uncertainty in t_{cs} and t_{is} is in the order of 10%.

The propagation velocity of cable with wire earth screen is influenced by the length of lay. The lay length is rarely found in a data sheet. A typical lay length is 8-10 times the earth screen diameter. For this lay length an uncertainty of 10% results in an uncertainty of 1% in the velocity.

7 CONCLUSION

In this paper it is shown that the characteristic impedance Z_c and propagation velocity v_p of single-core and three-core XLPE cables can be estimated using data that is found in a typical datasheet. For single-core cables Z_c and v_p are estimated with an accuracy of a few percent. For three-core cables with common earth screen the accuracy of the estimation of Z_c of both methods is 5 to 10%. The accuracy of both methods in the v_p of the PP channel is similar to the accuracy of the estimation for single-core cables. For v_p of the SP channel, however, the conformal mapping estimation is significantly less accurate.

The sensitivity analysis on single-core cables shows that accurate values for the conductor radius and the shield radius

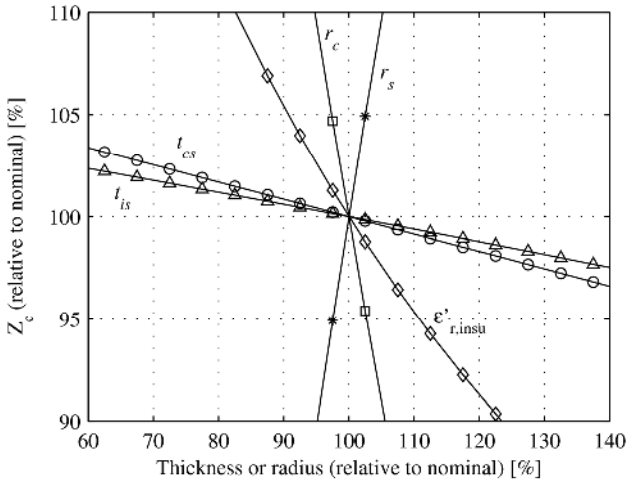

Figure 12. Relative change in characteristic impedance Z_c as a function of relative changes in t_{cs}, t_{is}, r_c, r_s and $\varepsilon'_{r,insu}$.

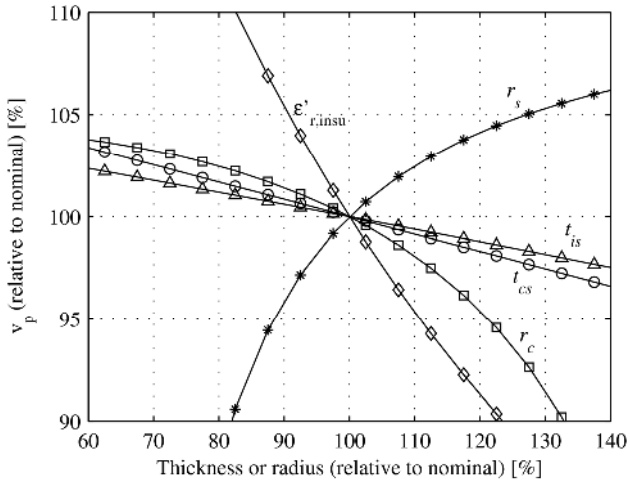

Figure 13. Relative change in propagation velocity v_p as a function of relative changes in t_{cs}, t_{is}, r_c, r_s and $\varepsilon'_{r,insu}$.

are most crucial for accurate modeling. The transmission line parameters are much less sensitive to variation in the thicknesses of the semiconducting layers.

APPENDIX

In order to decouple the normal voltages **V** and currents **I** (as defined in equations (5) and (6)) the transformation matrix **T** (as given in equation (9)) is applied. This gives the modal voltages $\mathbf{V_m}$ and currents $\mathbf{I_m}$:

$$\mathbf{V_m} = \mathbf{T}^{-1}\mathbf{V} = \frac{1}{\sqrt{3}}\begin{pmatrix} V_1+V_2+V_3 \\ V_1-\frac{1}{2}(V_2+V_3)+j\frac{1}{2}\sqrt{3}(V_3-V_2) \\ V_1-\frac{1}{2}(V_2+V_3)+j\frac{1}{2}\sqrt{3}(V_2-V_3) \end{pmatrix} \tag{38}$$

$$\mathbf{I_m} = \mathbf{T}^{-1}\mathbf{I} = \frac{1}{\sqrt{3}}\begin{pmatrix} I_1+I_2+I_3 \\ I_1-\frac{1}{2}(I_2+I_3)+j\frac{1}{2}\sqrt{3}(I_3-I_2) \\ I_1-\frac{1}{2}(I_2+I_3)+j\frac{1}{2}\sqrt{3}(I_2-I_3) \end{pmatrix} \tag{39}$$

Combining these with the voltages and currents of the SP and PP channels (respectively V_{sp}, $V_{pp,1}$, $V_{pp,2}$ and I_{sp}, $I_{pp,1}$, $I_{pp,2}$) as defined in equations (10) and (11) shows that they are related according:

$$\mathbf{V_m} = \begin{pmatrix} \sqrt{3}V_{sp} \\ \frac{1}{2}((j+\frac{1}{3}\sqrt{3})V_{pp,1}+(-j+\frac{1}{3}\sqrt{3})V_{pp,2}) \\ \frac{1}{2}((-j+\frac{1}{3}\sqrt{3})V_{pp,1}+(j+\frac{1}{3}\sqrt{3})V_{pp,2}) \end{pmatrix} \tag{40}$$

$$\mathbf{I_m} = \begin{pmatrix} \frac{1}{3}\sqrt{3}I_{sp} \\ (j+\frac{1}{3}\sqrt{3})I_{pp,1}+(-j+\frac{1}{3}\sqrt{3})I_{pp,2} \\ (-j+\frac{1}{3}\sqrt{3})I_{pp,1}+(j+\frac{1}{3}\sqrt{3})I_{pp,2} \end{pmatrix} \tag{41}$$

The modal characteristic impedance matrix $\mathbf{Z_{c,m}}$ gives the ratio between modal voltages and currents at any point in the transmission line. $\mathbf{Z_{c,m}}$ can be expressed in terms of the characteristic impedances of the SP and PP channels. From equations (40) and (41) the following expression is derived:

$$\mathbf{V_m} = \mathbf{Z_{c,m}}\mathbf{I_m} \quad \Rightarrow \quad \mathbf{Z_{c,m}} = \begin{pmatrix} 3Z_{sp} & 0 & 0 \\ 0 & \frac{1}{2}Z_{pp} & 0 \\ 0 & 0 & \frac{1}{2}Z_{pp} \end{pmatrix} \tag{42}$$

where Z_{sp} the characteristic impedance of the SP channel ($= V_{sp}/I_{sp}$) and Z_{pp} the characteristic impedance of both PP channels ($= V_{pp,1}/I_{pp,1} = V_{pp,2}/I_{pp,2}$). Substituting $\mathbf{V_m}$ and $\mathbf{I_m}$ with $\mathbf{T^{-1}V}$ and $\mathbf{T^{-1}I}$ and substituting $\mathbf{Z_c} = \sqrt{(\mathbf{ZY^{-1}})}$ yields:

$$\mathbf{Z_{c,m}} = \mathbf{T}^{-1}\mathbf{Z_c}\mathbf{T} = \mathbf{T}^{-1}\sqrt{\mathbf{ZY}^{-1}}\mathbf{T} \tag{43}$$

The relation between Z_{sp} and Z_{pp} and the mutual and self impedances and admittances is found by combining equation (42) with equation (43) and substituting equation (7) for **Z** and **Y**:

$$Z_{sp} = \frac{1}{3}\sqrt{\frac{2Z_m+Z_s}{2Y_m+Y_s}} \tag{44}$$

$$Z_{pp} = 2\sqrt{\frac{Z_m-Z_s}{Y_m-Y_s}} \tag{45}$$

The modal propagation matrix $\boldsymbol{\gamma}_\mathbf{m}$ gives the relation between the modal voltage/current at a certain location and the modal voltage/current at distance z from that location. From equations (40) and (41) the following expression is derived:

$$\left.\begin{aligned} \mathbf{V_m}(z) &= \mathbf{e}^{-\boldsymbol{\gamma}_\mathbf{m} z}\mathbf{V_m}(0) \\ \mathbf{I_m}(z) &= \mathbf{e}^{-\boldsymbol{\gamma}_\mathbf{m} z}\mathbf{I_m}(0) \end{aligned}\right\} \quad \Rightarrow \quad \boldsymbol{\gamma}_\mathbf{m} = \begin{pmatrix} \gamma_{sp} & 0 & 0 \\ 0 & \gamma_{pp} & 0 \\ 0 & 0 & \gamma_{pp} \end{pmatrix} \tag{46}$$

where γ_{sp} is the propagation coefficient of the SP channel and γ_{pp} the propagation coefficient of the PP channel. The relation between

$\boldsymbol{\gamma}_\mathbf{m}$ and the impedance and admittance matrices **Z** and **Y** is:

$$\boldsymbol{\gamma}_\mathbf{m} = \mathbf{T}^{-1}\boldsymbol{\gamma}\mathbf{T} = \mathbf{T}^{-1}\sqrt{\mathbf{ZY}}\mathbf{T} \tag{47}$$

The relation between γ_{sp} and γ_{pp} and the mutual and self impedances and admittances is found by combining equation (46) with equation (47) and substituting equation (7) for **Z** and **Y**:

$$\gamma_{sp} = \sqrt{(2Z_m + Z_s)(2Y_m + Y_s)} \tag{48}$$

$$\gamma_{pp} = \sqrt{(Z_m - Z_s)(Y_m - Y_s)} \tag{49}$$

The propagation velocities of the SP and PP channels can be found using equation (4):

$$v_{sp} = \frac{\omega}{\mathrm{Im}(\gamma_{sp})} \quad \text{and} \quad v_{pp} = \frac{\omega}{\mathrm{Im}(\gamma_{pp})} \tag{50}$$

ACKNOWLEDGMENT

The authors wish to thank KEMA Nederland B.V. and the Dutch utilities Liander N.V., Stedin B.V. and ENEXIS B.V. for supporting this research.

REFERENCES

[1] G.C. Stone and S.A. Boggs, "Propagation of partial discharge pulses in shielded power cable", IEEE Conf. Electrical Insulation and Dielectric Phenomena (CEIDP), Amherst, MA, USA, pp. 275-280, 1982.

[2] W.L. Weeks and Y.M. Diao, "Wave propagation characteristics in underground power cable", IEEE Trans. Power App. Syst., Vol. 103, pp. 2816-2826, 1984.

[3] G. Mugala, R. Eriksson, U. Gäfvert and P. Pettersson, "Measurement Technique for High Frequency Characterization of Semi-conducting Materials in Extruded Cables", IEEE Trans. Dielectr. Electr. Insul., Vol. 11, pp. 471-480, 2004.

[4] G. Mugala, R. Eriksson and P. Pettersson, "Dependence of XLPE insulated power cable wave propagation characteristics on design parameters", IEEE Trans. Dielectr. Electr. Insul., Vol. 14, pp. 393-399, 2007.

[5] S.R. Seshadri, *Fundamentals of transmission lines and electromagnetic fields*. London, UK: Addison-Wesley, 1971.

[6] C.R. Paul, *Analysis of multiconductor transmission lines*. Chichester, UK: Wiley, 1994.

[7] C.R. Paul, "Decoupling the multiconductor transmission line equations", IEEE Trans. Microw. Theory Tech., Vol. 44, pp. 1429-1440, 1996.

[8] C. Xu and S.A. Boggs, "High Frequency Properties of Shielded Power Cable Part 2: Sources of Error in Measuring Shield Dielectric Properties", IEEE Electr. Insul. Mag., Vol. 22, No. 1, pp. 7-13, 2006.

[9] S. Boggs, A. Pathak and P. Walker, "Partial Discharge XXII: High Frequency Attenuation in Shielded Solid Dielectric Power Cable and Implications Thereof for PD Location", IEEE Electr. Insul. Mag., Vol. 12, No. 1, pp. 9-16, 1996.

[10] G. Mugala, R. Eriksson and P. Petterson, "Comparing Two Measurement Techniques for High Frequency Characterization of Power Cable Semi-conducting and Insulation Materials", IEEE Trans. Dielectr. Electr. Insul., Vol. 13, pp. 712-716, 2006.

[11] D.A. Hill and J.R. Wait, "Propagation Along a Coaxial Cable with a Helical Shield", IEEE Trans. Microw. Theory Tech., vol. 28, no. 2, pp. 84-89, Feb., 1980.

[12] R. Papazyan, P. Pettersson and D. Pommerenke, "Wave Propagation on Power Cables with Special Regard to Metallic Screen Design", IEEE Trans. Dielectr. Electr. Insul., Vol. 14, pp. 409-416, 2007.

[13] Y.B. Yildir and B.M. Klimpke, "Calculation of transmission line parameters with the boundary element method", Symp. Antenna Technology and Applied Electromagnetics (ANTEM), Winnipeg, Manitoba, Canada, 1988.

[14] R. Schinzinger and A. Ametani, "Surge propagation characteristics of pipe enclosed underground cables", IEEE Trans. Power App. Syst., Vol. 97, pp. 1680-1688, 1978.

[15] A. Semlyen and D. Kiguel, "Phase parameters of pipe type cables", IEEE PES Winter Meeting, New York, USA, paper No. A 78 001-0., 1978.

[16] J. Bajorek, "Admittance and impedance matrices of multiconductor power cables – Application of Poynting's theorem", Intern. J. of Elect. Power & Energy Syst., Vol. 7, No. 2, pp. 120-126, 1985.

[17] R. Papazyan and R. Eriksson, "Calibration for Time Domain Propagation Constant Measurements on Power Cables", IEEE Trans. Instrum. Meas., Vol. 52, pp. 415-418, 2003.

[18] J. Yang, R. Huang and D. Zhang, "A Field-circuit Coupled Method to Accurately Determine Intrinsic Complex Permittivity of XLPE Insulation Material", IEEE Trans. Dielectr. Electr. Insul., Vol. 15, pp. 334-341, 2008.

[19] P. Wagenaars, P.A.A.F. Wouters, P.C.J.M. van der Wielen and E.F. Steennis, "Approximation of Transmission Line Parameters of Single-Core XLPE Cables", IEEE Intern. Symp. Elect. Insul. (ISEI), pp. 20-23, 2008.

Paul Wagenaars (S'06) was born in Schaijk, The Netherlands in 1981. He received the M.Sc. degree in electrical engineering from the Eindhoven University of Technology, Eindhoven, The Netherlands in 2004. After his graduation he worked at KEMA on advanced calculation techniques for the current carrying capacity of power cables. Since 2006 he has been pursuing the Ph.D. degree. His current research mainly deals with online partial discharge monitoring of medium-voltage cable systems.

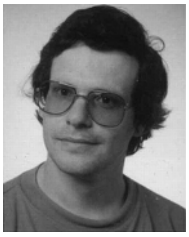

Peter A.A.F. Wouters was born in Eindhoven, The Netherlands, on 9 June 1957. He studied physics at the Utrecht University (UU), Utrecht, The Netherlands, until 1984, from which he received the Ph.D. degree for a study on elementary electronic transitions between metal surfaces and low energetic (multiple) charged ions in 1989. In 1990, he joined the Electrical Power Systems (EPS) group at the Technical University of Eindhoven, Eindhoven, The Netherlands, as Research Associate. His research interests include partial discharge techniques, vacuum insulation, and LF electromagnetic field screening. Currently, he is an Assistant Professor in the field of diagnostic techniques in high-voltage systems.

Peter C.J.M. van der Wielen (M'93) was born in Hulst, the Netherlands, on 6 March 1973. He studied electrical engineering at the Eindhoven University of Technology (EUT), where he was also a member of the board and of many committees of the IEEE Student Branch Eindhoven. He received the M.Sc. degree in 2000. After that he started doing research on power cable diagnostics at both the Electrical Power Systems group at this university and KEMA, Transmission and Distribution Testing Services, in the Netherlands. In 2005 he received the Ph.D. degree for his study on on-line detection and location of PDs in medium voltage power cables. Since then he works as a consultant/specialist on power cables at KEMA. Subjects in the field of work are: power cable diagnostics, power cable consultancy in general, asset management, development of new measuring techniques & diagnostic methods and failure analysis. Furthermore, he is one of the lecturers of the KEMA Power Cable Courses.

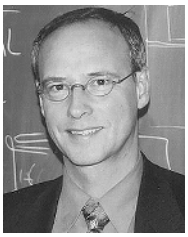

E. Fred Steennis joined KEMA, Arnhem, The Netherlands, in 1982, after his education at the Eindhoven University of Technology, Eindhoven, The Netherlands, where he studied degradation mechanisms in energy cables for the Dutch utilities. It was on this subject that he received the doctor's thesis from the Technical University in Delft, Delft, The Netherlands, in 1989. In and outside the Netherlands, he is a consultant on energy cables and is the author and a teacher of the KEMA course on Power Cables. At KEMA, he is currently a senior consultant. Since 1999, he has also been a part-time Professor at the Technical University in Eindhoven, where he teaches and studies diagnostics for power cables. Prof. Dr. Ir. Steennis received the Hidde Nijland award for his contributions in 1991. After that, his experience on degradation mechanisms and related test methods both in the field and the laboratory was further enhanced. Based on this expertise, he became the Dutch representative with the Cigré Study Committee on High-Voltage Cables. He is also a member of various international Working Groups.